Progress In Electromagnetics Research, Vol. 122, 245–268, 2012

A NEW UNMANNED AERIAL VEHICLE SYNTHETIC APERTURE RADAR FOR ENVIRONMENTAL MONITORING

V. C. Koo[1], Y. K. Chan[1,*], V. Gobi[1], M. Y. Chua[1], C. H. Lim[1], C. S. Lim[1], C. C. Thum[1], T. S. Lim[1], Z. Ahmad[2], K. A. Mahmood[2], M. H. Shahid[2], C. Y. Ang[1], W. Q. Tan[1], P. N. Tan[1], K. S. Yee[1], W. G. Cheaw[1], H. S. Boey[1], A. L. Choo[1], and B. C. Sew[1]

[1]Faculty of Engineering & Technology, Multimedia University, Jalan Ayer Keroh Lama, Bukit Beruang, Melaka 75450, Malaysia

[2]Malaysian Remote Sensing Agency, No. 13, Jalan Tun Ismail, 50480 Kuala Lumpur, Malaysia

Abstract—A new Unmanned Aerial Vehicle (UAV) Synthetic Aperture Radar (SAR) has been developed at Multimedia University, in collaboration with Agency of Remote Sensing Malaysia. The SAR operates at C-band, single VV-polarization, with $5\,\mathrm{m} \times 5\,\mathrm{m}$ spatial resolution. Its unique features include compact in size, light weight, low power and capable of performing real-time imaging. A series of field measurements and flight tests has been conducted and good quality SAR images have been obtained. The system will be used for monitoring and management of earth resources such as paddy fields, oil palm plantation and soil surface. This paper reports the system design and development, as well as some preliminary results of the UAVSAR.

1. INTRODUCTION

Radar is the abbreviation for "Radio Detection and Ranging". It operates by radiating electromagnetic energy through a transmitting antenna and detecting the reflected or scattered signal from the target [1]. SAR is an imaging radar which utilizes relative motion between an antenna and the target under observation to *synthesize* a very long antenna via signal processing [2]. As compared to

Received 26 September 2011, Accepted 2 November 2011, Scheduled 18 November 2011

* Corresponding author: Yee Kit Chan (ykchan@mmu.edu.my).

the conventional real aperture radar, SAR can obtain finer spatial resolution particularly in azimuth direction. The concept of SAR can be traced back to early 1950s when Carl Wiley proposed a Doppler beam sharpening system to improve the azimuth resolution of radar [3, 4]. Today, SAR has become an important tool for microwave remote sensing because of its capability to operate day and night, and in nearly all weather conditions [5]. It has wide range of applications, including sea and ice monitoring [6], mining [7], oil pollution monitoring [8], oceanography [9], snow monitoring [10], terrain classification [11] and so on. The potential of SAR in a diverse range of applications has led to the development of a number of airborne and spaceborne SAR systems.

An *unmanned aerial vehicle (UAV)* is an unpiloted aircraft typically found in the area of surveillance, reconnaissance as well as military missions. The earliest UAV was found in 1916 [12], followed by a number of remote-controlled airplanes developed during and after World War I for military applications. UAV is currently one of the mostrapid growth research areas due to its increased importance in military operations [13]. The role of a UAV system falls mainly in reconnaissance and surveillance missions that utilize remote sensing instruments such as electro-optical (EO) sensors, infrared (IR) sensors and synthetic aperture radars (SAR). The increased popularity of a UAV system compared to a conventional aircraft is due to a few factors. There is no risk of losing human life especially for risky operations. The over loading of a manned aircraft has to be limited to 10 g due to human physical limitations but it can be increased up to 20 g for UAV. There is also no concern on human fatigue and boredom in a long UAV mission. The weight of the human pilots is roughly equivalent to 15% of the effective load of a military aircraft, while the pilot related supporting and emergency systems cost as much as 50% of the total cost of the aircraft [13]. Therefore the size of a UAV is only about 60% of the size of a manned aircraft with the same performance and the price for a UAV system is expected to be 40% less than the cost of a manned solution [13, 14].

In terms of remote sensing applications, UAV-based imaging radar such as SAR has great potential due to its all-day, all-weather capabilities. As compared to conventional airborne or space-borne SAR systems, UAV SARs have several advantages which include low cost, low risk and timely operations.This has led to the development of a number of UAV SAR systems in recent years.

A low cost, compact and low power micro-SAR (μSAR) system has been developed by the Brigham Young University (BYU) [15]. The μSAR is based on a linear frequency modulated continuous

wave (LFM-CW) configuration, which has smaller size and power requirements as compared to a conventional pulsed SAR system. This enables the BYU μSAR to fly on a small UAV, further reducing the cost of operation. The μSAR was designed to image Arctic sea ice. The target UAV has a 6-foot wingspan, flies at low-altitudes (< 300 m), with limited power to supply to the payload. European Aeronautic Defence and Space Company (EADS) has developed a miniaturised SAR (MISAR) sensor that was specially designed for UAVs with stringent payload size, weight and power (SWP) constraints. The LUNA UAV of the German manufacturer EMT was chosen as the reference platform. LUNA has a take-off weight in the order of 35 kg and its payload weight is restricted to 4 kg. The flying altitude of LUNA is between 300–2000 m with the velocity of 10–40 m/s. This UAVSAR will be operated at stripmap mode with swath width of 500–1000 m. In order to achieve SWP requirement, the FMCW configuration is employed. The Jet Propulsion Laboratory (JPL) has designed and developed a L-band SAR for repeat pass deformation measurements on a UAV platform [16–18]. The SAR system is operated at a wavelength of 0.2379 m (L-band, 1.26 GHz) and bandwidth of 80 MHz. The pulse duration is designed at 40 msec with PRF of 350 Hz (interleaving H and V transmit polarizations). It is a fully polarimetric and repeat pass interferometry SAR system. The UAVSAR is able to obtain a range swath of 16 km with look agle of 30 to 60 degree. The system will nominally operate at 45,000 ft. Both ALTAIR and the Proteus can be used for this SAR system.

Research Establishment for Applied Science (FGAN) is in the progress of developing ARTINO (Airborne Radar for Three dimensionally Imaging and Nadir Observation) [19–21]. It comprises a low flying UAV, which will be able to map a directly overflown scene into a high resolution three-dimensional image by looking perpendicularly downward. With a wingspan of only 4m and a modular structure the UAV can be split up into small segments and easily transported to the area of interest. Due to the light weight of only 25 kg it is possible to fly at a slow speed of approximately 15 m/s. Since ARTINO is a low flying UAV, the 3D imaging radar can be designed for short range. Hence, the average transmitting power is only a few Watts.

A commercial available UAVSAR — Lynx SAR has developed by Sandia National Laboratories [22, 23]. Lynx is a state-of-the-art, ultra-fine-resolution, real-time *SAR* and ground moving target indicator (GMTI) radar. Sandia National Laboratories collaborated with General Atomics (GA) to design and build the Lynx system to incorporate General Atomics' design requirements for operation

on their Predator, IGNAT, or Prowler II unmanned aerial vehicles (UAVs). AN/APY-8 Lynx II is a lightweight version of Lynx operating on the US Air Force Predator RQ-1 UAV. Lynx is a Ku-band multimode radar. Its SAR modes include real-time 0.1 m resolution spotlight and 0.3 m resolution stripmap modes. The radar can also scan a large or small area for moving objects, detecting targets at speeds typical of vehicular movements (10–70 kph). The Lynx SAR operates in the Ku-Band anywhere within the range 15.2 GHz to 18.2 GHz, with 320 W of transmitter power.

Many other UAVSAR systems are designed for government agency, research institution and private industry. An experimental millimetre band (34 GHz frequency) Synthetic Aperture Radar (SAR) sensor has been developed by Polytechnic University of Madrid, Spain [24]. It is a short-range (2 Km) high-resolution (30×30 cm^2) SAR system with bandwidth of 675.8 MHz and PRF of 1300 Hz. Research Institute of China Electronics Technology Group Corporation is also designed a 35 GHz, 8 mm wavelength UAV-borne SAR [25]. The resolution achieved by this UAVSAR is proved by flight experiments that have reached 0.85 m × 0.45 m. A Ka band, fully-polarized SAR radar is developed by the Lincoln Laboratory. This millimeter-wave SAR imaging system has the bandwidth of 600 MHz in order to assure 0.3 m range resolution. The strip is 440 m wide, the spot imaging area is 150 m × 150 m, and the azimuth resolution is 0.3 m [25]. Italy Salenia Corporation has developed a UAV-borne MMW SAR which can perform ground mapping, detection, tracking and imaging of slow-speed objects. The operating frequency is 35 GHz. The SAR system weight 60 kg and takes up 0.05 m^3. The waveguide slotted antenna is 1 m long, 0.24 m wide and 2 kg weight. Pulse width 6 μs and bandwidth is 40 MHz. The range resolution corresponding to the pulse compression is 5 m. Microwave Remote Sensing Laboratory, Center for Environmental Remote Sensing, Chiba University is currently developing its Circular Polarization SAR (CP-SAR) sensor which can be used in UAV as well as satellite based platform [26]. This sensor is operated with center frequency on L band (1.27 GHz) and 10 MHz of chirp pulse bandwidth. The sensor is designed as a low cost, simple, light, strong, low power, low profile configuration to transmit and receive left-handed circular polarization (LHCP) and right-handed circular polarization (RHCP), where the transmission and reception are working in RHCP and RCHP + LCHP, respectively.

In late 2008, a new UAVSAR project was initiated at Multimedia University (MMU), Malaysia, in collaboration with Agency Remote Sensing of Malaysia (ARSM). This project was started after preparatory studies in the previous year [27–31]. The proposed system

is a C-band, VV-polarization, miniature SAR mounted on a small UAV. The UAVSAR system is designed to operate at low altitudes with low transmit power in order to optimize the operating cost. The construction of the SAR sensor was completed in early 2010. A series of indoor and outdoor testing and measurements has been carried out to verify the performance of the system. At the end of 2010, flight missions have been conducted at Mersing, Johor. High quality SAR images were obtained which demonstrated the capabilities of the UAVSAR for remote sensing applications in Malaysia.

This paper presents the system design and development, as well as some preliminary results of the UAVSAR. Section 2 outlines the major design issues and considerations for UAVSAR. Section 3 describes the development of various SAR subsystems including the microstrip patch antenna, the radar electronics, the embedded SAR controller and processor, and the UAV platform. Section 4 presents some of the preliminary results obtained by the UAVSAR, which include ground-based SAR experiments and fight tests. Finally, Section 5 concludes the paper.

2. DESIGN CONSIDERATIONS

The primary goal of this research project is to develop an UAV based SAR system which capable to illuminate terrain and construct the image of the scanned area. High level design consideration have been carefully considered and presented in this section.

2.1. Operating Frequency

C-band (4–8 GHz) frequency is widely used for high-resolution land imaging, agricultural monitoring and ocean observations. In this frequency band, incident wave tends to be reflected more by vegetation canopies rather than the surface layer. This penetration characteristic allows the canopy biomass and soil below the canopy to be analyzed. The center frequency of the UAVSAR is selected at 5.3 GHz, which is within the allowable spectrum (5250–5460 MHz) defined by International Telecommunication Union (ITU) for Earth Exploration Satellite System (EESS) [32]. Beside the reason of having low absorption in the atmospheric-window region, the size of a C-band antenna is considerably small and most of the RF components are easily available.

2.2. Mode of Operation

The two most common SAR imaging modes are stripmap and spotlight. The stripmap is a standard mode of SAR operation, widely used by airborne SAR sensors where a strip (swath) to the side of the aircraft is imaged. On the other hand, a spotlight SAR steers its antenna beam to continuously illuminate a specific terrain patch during data collection. The spotlight mode is suitable to collect fine-resolution data from localized areas, while the stripmap mode is more efficient when used for coarse-resolution mapping of large regions. In our design, the stripmap mode is the preferred choice.

2.3. Polarization

Single polarization mode is proposed for simple classification and multi-temporal change detection. VV-polarization is the preferred configuration since it is sensitive to the vegetation's vertical canopy structure, thus providing the opportunity for crop type and growth stage discrimination.

2.4. Dynamic Range

Based on the measurement results reported in numerous literatures, it is found that typical values of scattering coefficients for various categories of terrain fall in the range from 0 dB to -30 dB [33]. Therefore, a wide dynamic range (> 30 dB) is needed to accommodate the measurement of various types of terrain.

2.5. Resolution

Typical resolution of airborne SAR ranges from 1 m to 20 m. It depends mostly on the application requirements. Since the main objective is to monitor earth resources such as vegetation fields, resolution of $5\,\text{m} \times 5\,\text{m}$ for both range and azimuth direction will be adequate.

2.6. Antenna Requirements

A planar, lightweight, small size, linearly polarized microstrip patch array panel is proposed. The center frequency for the array is set at 5.3 GHz, with more than 80 MHz bandwidth. The directive gain of the panel should be more than 15 dBi for good detection in the presence of noise. Due to the limited space of the UAV platform, the antenna will be mounted directly underneath the fuselage. The beamwidth will be tilted 25° off nadir for side-looking operation.

2.7. Signal Processor

The on-board facility consists of a high-speed analog-to-digital converter, a front-end processor, and a high-density digital data recorder to store the raw data. The SAR images should be produced by both ground processing facility and onboard processor. Real-time data capturing, recording and processing are desired for timely monitoring during flight mission.

2.8. Motion Sensing

The irregular motion of the aircraft due to atmospheric turbulence will seriously affect the image quality. In particular, the change of altitude causes the image out of focus. In this system, an embedded inertial navigation system (INS) and global positioning system (GPS) are used to provide integrated flight information.

2.9. UAV Platform

A small UAV will be used to install the radar system. The platform should support true ground speed of approximately 30–40 m/s with operating altitude at about 1000 m. The desired payload is at least 20 kg.

The constraints that are imposed onto the design of the remote sensing instruments for UAVs are mainly weight, power consumption and volume. The aircraft should have a lot of reserve internal volume and electrical power so that it is well-suited for a variety of payloads. The SAR system can be designed to fit existing EO/IR sensor mounting as the mounting will become common for remote sensing platform and it certainly helps interpretability. The UAV performance such as flight speed and altitude also dictate the design of the SAR system. In this project, Aludra MK1 has been chosen as the SAR platform.

Figure 1. Aludra MK1.

Aludra MK1 is developed by UST (Unmanned Systems Technology), Malaysia with the dimension of 4.27 m and wingspan of 4.88 m. The image of Aludra MK1 is shown in Figure 1. The typical speed of MK1 is 35 m/s and up to maximum speed of 61 m/s. Endurance of this UAV is about 3 hrs. However limited payload weight is a challenge. The working space is about 27 cm $(W) \times 35$ cm $(L) \times 25$ cm (H) and maximum payload of 20 kg. Thus extra attentions need to be taken for the dimension and weight of the SAR sensor and antenna size. Therefore a new chassis of the SAR sensor need to be design and constructed for installing all SAR subsystem.

Based on the design considerations described above, the specifications of the UAVSAR system are determined and are summarized in Table 1. Figure 2 shows the geometric configuration of the UAVSAR. The standard image size produced is 900 m (range) by 1500 m (azimuth).

Table 1. UAVSAR system specifications.

System Parameters	**Specifications**
Mode of Operation	Stripmap
Operating Frequency	5.3 GHz (C-band)
Modulation	LFM Pulse
Bandwidth	80 MHz
Pulse Repetition Frequency	1000 Hz
Pulse Width	10 µs
Polarization	VV
Antenna Gain	15 dBi
Antenna Size	1 m × 0.3 m
Spatial Resolution	5 m × 5 m
RCS Dynamic Range 30 dB	0 dB to −30 dB
SNR	> 10 dB
Platform Height, h	1000 m
Swath Width	900 m
Nominal Platform Speed	35 m/s
Data Take Duration	1–2 hour (50 sec per scene)
Operating Platform	UAV, Aludra MK1
Overall Sensor Weight	< 20 kg
Overall Sensor Dimension	$<$27 cm $(W) \times 35$ cm $(L) \times 25$ cm (H)
Peak Transmit Power	50 W

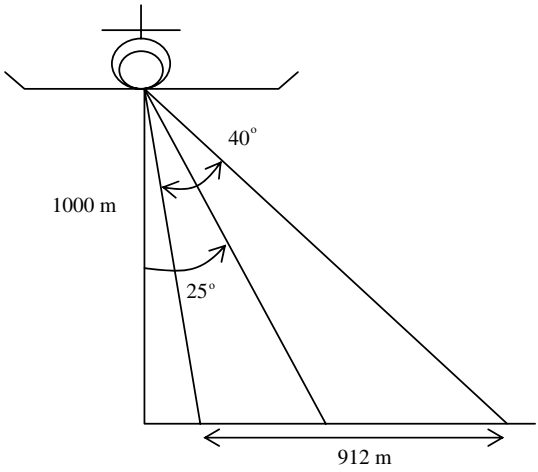

Figure 2. Geometric configuration of the UAVSAR system.

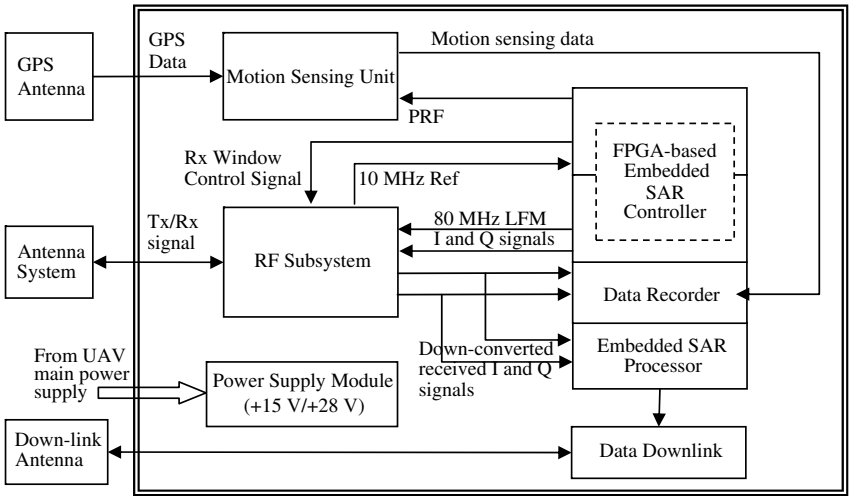

Figure 3. Functional block diagram of the SAR sensor.

3. SYSTEM IMPLEMENTATION

Figure 3 shows the functional block diagram of the UAVSAR Sensor.

In this design, a Field-Programmable Gate Array (FPGA) based SAR controller is used to produce the required linear FM (LFM) signals and other necessary timing signals. The LFM I and Q signals are up-converted and amplified in the RF subsystem before transmitting

out via an antenna system. The antenna system is implemented by using microstrip patch arrays. The returned echoes are amplified and down-converted into an intermediate frequency (IF), at which they are further digitized and stored in the data recorder. A replica of the IF signal is fed into an embedded SAR processor for real-time image formation. The resultant image will be transmitted to the ground station via a 2.4 GHz data downlink unit. An integrated Inertial Measurement Unit (IMU) with Global Positioning System (GPS) receiver is also developed to provide the necessary platform motion information.

3.1. RF Subsystem

The block diagram of the RF subsystem is shown in Figure 4. Basically it can be divided into two sub-sections: the transmitter and the receiver. At the transmitter front-end, the I (In-phase) and the Q (quadrature-phase) chirp signals are mixed with the carrier frequency (5.3 GHz) via an up-convert mixer. The output of the mixer is amplified by a power amplifier (PA). A RF switch is used to turn on the transmitting window, where its on-time duration is selectable based on mission requirements. The signal is then fed to a bandpass filter to reject unwanted signal outside the desired frequency band, and further amplified by a high power amplifier (HPA) to boost up the power for long range transmission. The average output power is about 160 mW for nominal operating range of 1 km.

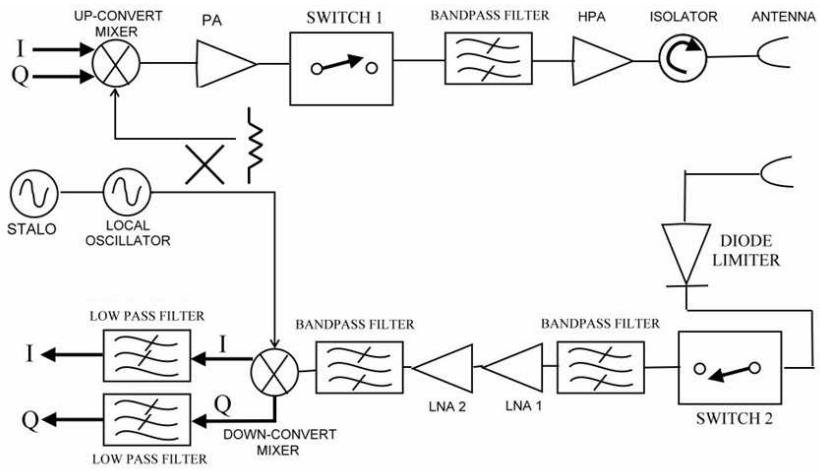

Figure 4. Functional block diagram of the SAR RF subsystem.

At the receiver front-end, a diode limiter is used to provide protection for any sudden power spikes from the transmission. A fast switching pin diode switch is employed to turn on the receiving window at certain range-gate interval, and to prevent saturation due to leakage signals from the transmitter. Two low noise amplifiers (LNAs) are cascaded to provide sufficient amplification for the returned echoes. Finally, the mixer down-converts the received signal to IF I and Q signals. The prototype of the RF subsystem is shown in Figure 5.

3.2. Antenna

The technical specifications of the SAR antenna are summarized in Table 2. Design and fabrication of the antenna is based on composite laminates. The antenna is fabricated as a single layer system whereby the patches and the feeds are assembled on one side of the surface, while the base of the plate attached to the undercarriage of the UAV will act as the ground plane.

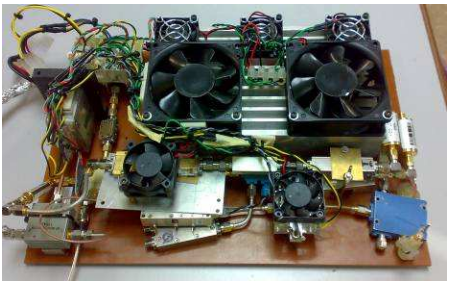

Figure 5. Prototype of the SAR RF subsystem.

Table 2. Antenna technical specifications.

System Parameters	Specifications
Operating Frequency	5.3 GHz (C-band)
Bandwidth	80 MHz
Polarization	VV
Antenna Gain	15 dBi
Platform Height, h	1000 m
Incident Angle	25°
Azimuth Beamwidth	4°
Elevation Beamwidth	40°

The UAVSAR antenna operates at 5.3 GHz with bandwidth of 80 MHz and transmits signal in single V polarization. This antenna adopts 3 layers configuration with the top layer acts as radiating layer, middle layer acts as ground plane with feeding network is designed on bottom layer. Probe fed method has been utilized where the EM signal is fed from feeding network to radiating elements through a probe. The UAVSAR antenna is divided into 3 sub panels for the ease of fabrication and then joined by power dividers. The back and front views of the final antenna system are depicted in Figures 6 and 7, respectively.

The azimuth array is formed with 24 radiating elements to produce a narrow pencil beam of 3°. The elevation radiation pattern of the antenna shows the main lobe is located at 30° away from center with beamwidth of 24° to provide wider swath width. Before it can be installed for flight mission, the performance of the antenna has been verified in the laboratory via VNA as well as radiation pattern measurement using anechoic chamber. The measured result shows the return loss value at 5.3 GHz achieve −32.381 dB. From the radiation pattern, the highest power level of sidelobe appears at −45° to −55° with the maximum sidelobe power level of −15 dB which help to overcome left-right ambiguity issue. Figure 8 shows the radiation pattern of the antenna which is well match with our simulation result.

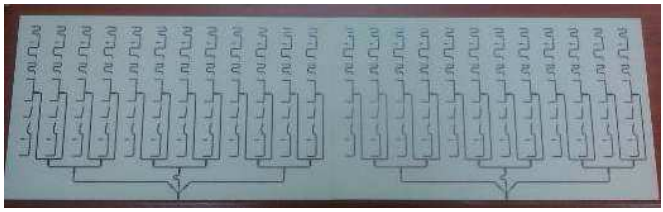

Figure 6. Back view of the fabricated antenna.

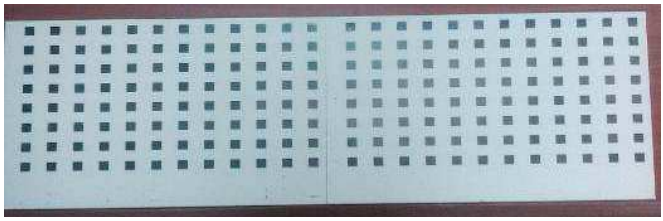

Figure 7. Front view of the fabricated antenna.

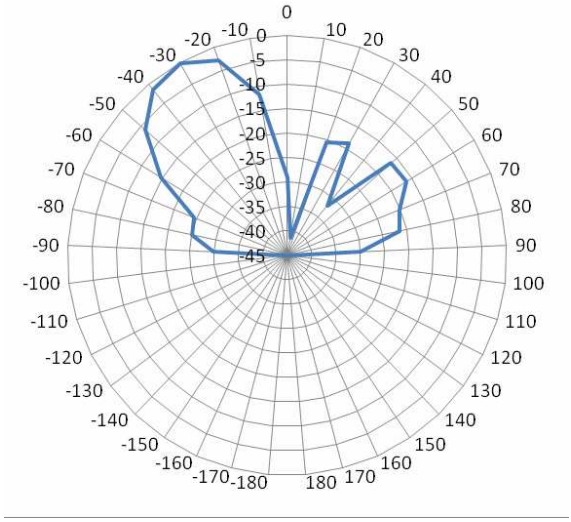

Figure 8. Measured radiation pattern of SAR antenna.

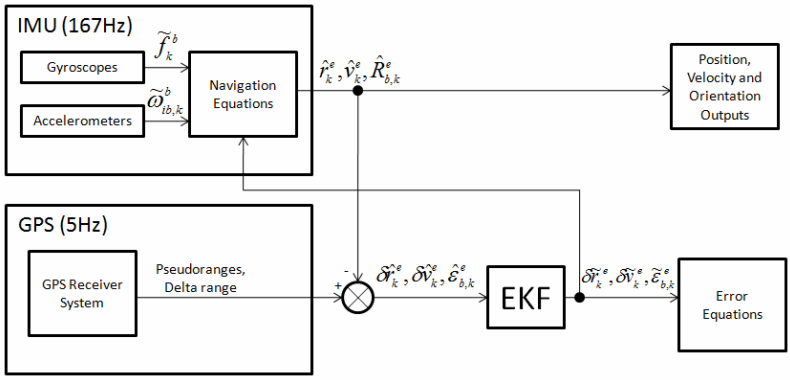

Figure 9. Block diagram of SAR motion sensing unit.

3.3. Motion Sensing Unit

An embedded motion sensing unit has been developed to collect the required information for motion compensation. These include data such as time, longitude, latitude, altitude, 3-axis accelerations and 3-axis angular velocity (raw, pitch and yaw). The block diagram of the SAR motion sensing unit is illustrated in Figure 9. The motion sensing of SAR sensor is achieved by integrating both global positioning

system (GPS) and strapdown inertial moment unit (IMU). The GPS is able to provide instantaneous position data on the SAR sensor with no accumulation errors, but suffers a relatively low data rate (5 Hz). On the other hand, the strapdown IMU provides higher data rate (167 Hz) for position, velocity and orientation estimations, but are subject to sensor's accumulation errors. Thus, the integration of GPS and IMU suppresses the shortcomings of each individual system, namely, the GPS's low data rate and IMU's accumulation errors. Also, the integration combines the advantages of both systems, such as the high accuracy positioning data in GPS and the short term stability of IMU.

As shown in the block diagram of Figure 9, the data from GPS and IMU were compared and feed into an extended Kalman filter (EKF) for optimal errors prediction and estimation. The estimated errors will be used to correct the original measurements. Due to data rate inconsistency between IMU and GPS, the data fusion event will only take place when GPS data was available. In the event of no GPS data the IMU will correct itself using the last predicted errors. The constructed motion sensing unit is shown in Figure 10.

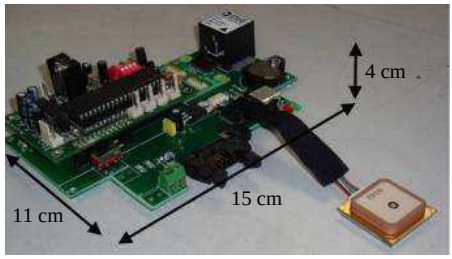

Figure 10. The integrated IMU-GPS motion sensing unit.

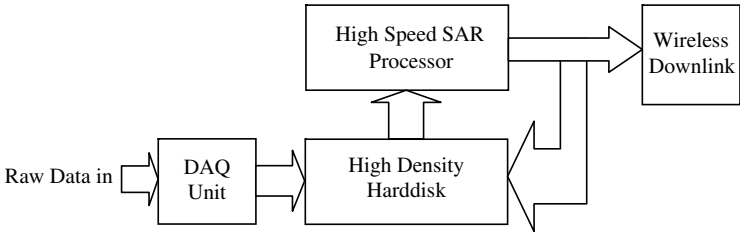

Figure 11. Overview of the embedded SAR processor and data recorder.

3.4. Embedded SAR Processor and Data Recorder

Figure 11 depicts the overview of the embedded SAR processor and data recorder. A high speed data acquisition unit (DAQ) is used to digitize the down-converted IF I and Q signals from the RF receiver. These raw data are directly stored onto a high density harddisk. Meanwhile, a sample of the stored data (level-0) will be retrieved from the storage and processed by the embedded SAR processor in real-time. The output of the on-board SAR processor is level-1 images, which will be sent to the ground receiving station via a wireless downlink.

There are a few stripmap mode imaging formation algorithms such as the Range Doppler algorithm (RDA), Chirp Scaling algorithm (CSA) and Wave Number Algorithm/Omega-K Algorithm (ωkA) [34]. RDA is a simple and mature SAR image processing algorithm with a relatively small amount of computation load and it is suitable for real-time processing. Basically, it divides the SAR echo signal processing into two one-dimensional processes in cascade, i.e., range compression followed by azimuth compression. In summary, real-time signal processing algorithms for airborne SAR can be implemented by RDA. RDA block diagram is shown in Figure 12. Therefore, RDA has been selected as the real time image formation algorithm for our UAVSAR system.

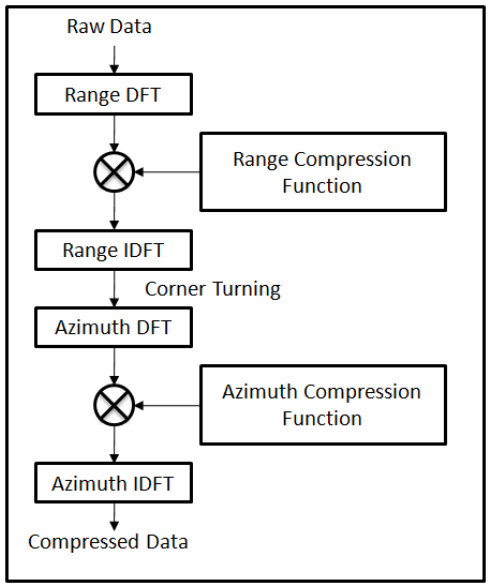

Figure 12. RDA block diagram.

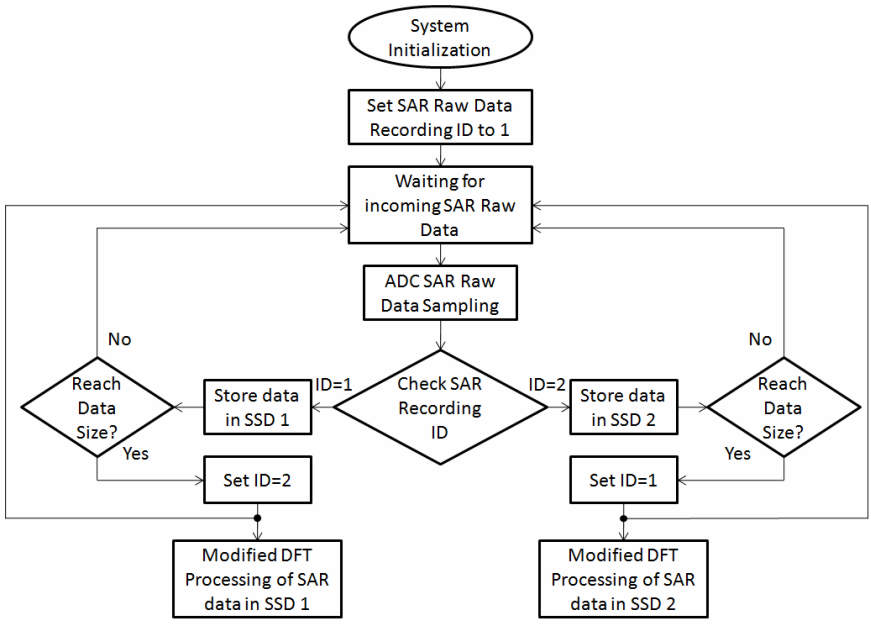

Figure 13. Block diagram of enhanced UAVSAR data recording and processing system.

The embedded SAR processor is implemented using a High Performance Computer (HPC). The selected motherboard has a Core2-based CPU and it is capable of supporting up to 4 GB of RAM. It also has a built-in CUDA (Compute Unified Device Architecture) compatible graphic processing unit. A 12-bit high-speed ADC card is employed for the implementation of the DAQ unit. This ADC card has two-channel inputs and it is capable of simultaneous sampling up to 250 MHz. The digitized data are transferred to the HPC via PCI express interface at 1.25 GBytes/s data rate. Figure 13 shows the block diagram of the enhanced UAVSAR data acquisition and processing system. It is worth mentioning that UAVSAR raw data is acquired using the ADC with a designed data rate of 7.5 Mbytes/s. After the conversion, the ADC stored the data in HPC's Random Access Memory (RAM) temporarily, where the HPC will excerpt the information out of the RAM and saved it into local mass storage device. Here lies the first bottleneck of the designed system, where a typical magnetic hard disk should not be used in UAV flight test due to the vibration of the flight might potentially damaged the hard disk's spinning disk with its read/write heads. This bottleneck can be resolve

by replacing the magnetic hard disk with solid-state drive (SSD). A SSD is a mass storage device uses microchip to store data. It contains no moving part during data retaining as compared to magnetic hard disk's spinning disk, and its data rate is also faster than magnetic hard disk. The second bottleneck lies on the physical data bus congestion in real time UAVSAR recording and processing application. However, enhancement can be made to resolve this bottleneck by proper arrangement of two SSDs into the system. As shown in Figure 13, the HPC is designed in such a way that the UAVSAR raw data recording and processing always taking place at different SSD, thus reducing the SSD's data bus congestion and enhancing the UAVSAR data processing efficiency.

3.5. System Installation

As shown in Figure 14, all the SAR subsystems except the antennas (SAR antenna, GPS antenna and data downlink antenna) are mounted inside the UAV compartment. The overall dimension of the SAR sensor is 27 cm $(W) \times 35$ cm $(L) \times 25$ cm (H), and the total weight of the system (SAR sensor plus antenna) is less than 20 kg. The SAR platform used is capable of operating at a nominal ground speed of 35 m/s at 1000 m. Figure 15 shows the bottom view of UAV platform, where the SAR antenna is placed directly underneath the UAV's fuselage.

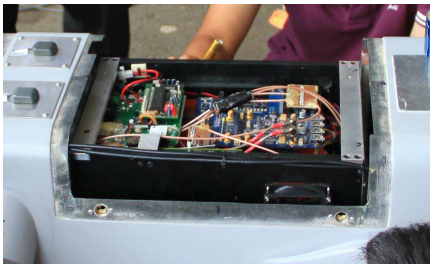

Figure 14. The SAR sensor mounted inside the UAV compartment.

Figure 15. The SAR antenna mounted at the bottom of the UAV's fuselage.

4. PRELIMINARY RESULTS

A series of field experiment has been conducted in year 2010 to verify the performance of the UAVSAR system. These include point target measurement, and ground-based SAR experiments using a moving platform. Flight tests were finally conducted at the end of 2010 to evaluate the overall performance of the SAR sensor.

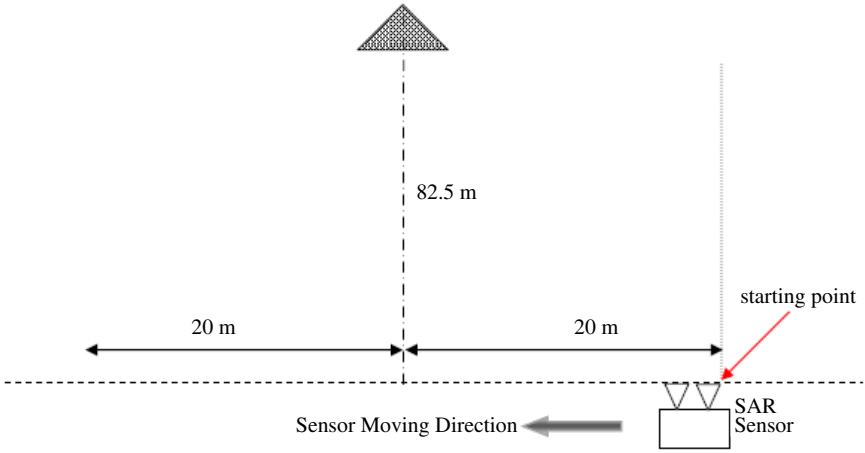

Figure 16. Experimental setup for point target measurement.

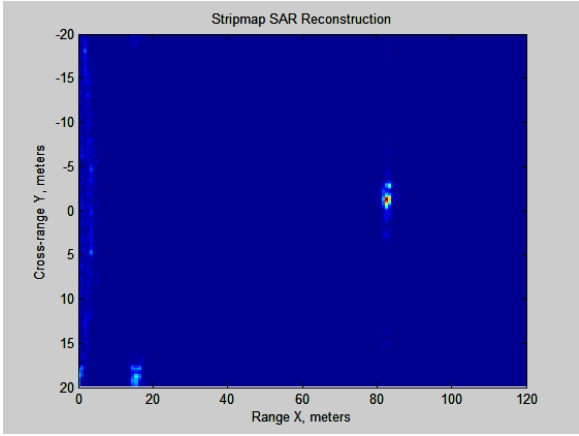

Figure 17. The SAR image of a trihedral placed at 82.5 m.

4.1. Point Target Measurement

Figure 16 shows the experimental setup for point target measurement. The test site was a public field with low background clutter. A trihedral corner reflector was placed on a polystyrene structure of about 1.5 m in height, located 82.5 m from the SAR transmitting antenna. The measurement was conducted by employing the *stop-and-go* approach, where the SAR sensor was manually moved to a pre-defined cross range (azimuth) position for every single range bin data capturing. The total cross range travelled was 40 m, which yields 400 points of azimuth data with 0.10 m spacing. Figure 17 shows a SAR image generated from this experiment. A strong target is clearly shown at location 82.5 m. The measured 3 dB azimuth resolution is 0.78 m, and the peak sidelobe level is -12.23 dB.

4.2. Ground-based SAR Experiment

In this experiment, the SAR system was mounted onto a truck. The truck was then travelled at a constant speed to perform SAR imaging. The target of interest was a housing area at distance (slant range) more than 1 km. Figure 18 shows the processed image where multiple strong targets are observed at distance more than 1 km. This preliminary ground experiment has successfully verified the overall imaging capability of the system.

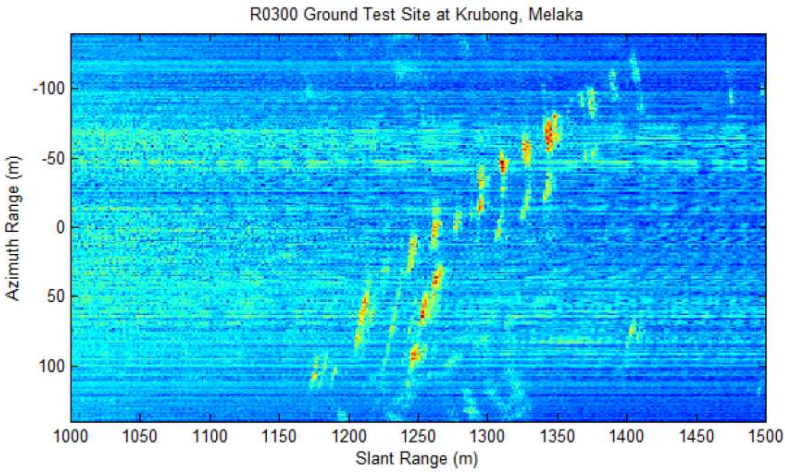

Figure 18. The SAR image of multiple targets (at distance > 1 km).

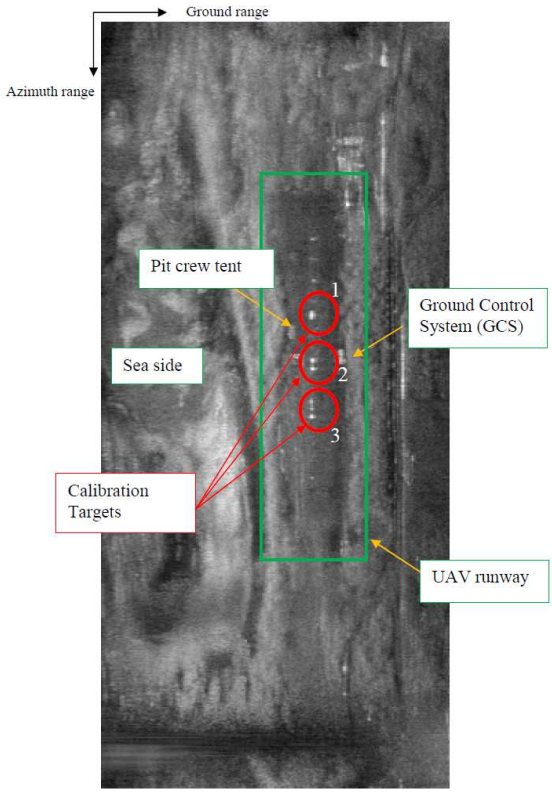

Figure 19. The SAR image of the calibration site at Mersing.

4.3. Fight Tests

Preliminary flight tests have been conducted in December 2010 at Mersing, Malaysia. During the 6-day flight mission, more than 200 sets of SAR raw data were collected. Eleven trihedral corner reflectors, arranged in three groups, were used as the point targets for external calibration. All the trihedral corner reflectors were placed in a straight line and perpendicular to the flight path of the UAV. Figure 19 shows the SAR image of the calibration site. Signatures such as the point targets, UAV runway, pit crew tent and ground control system are clearly observed.

Figures 20 and 21 show two samples of SAR images captured on Dec. 5th and Dec. 8th, 2010, respectively, with comparison to the Google Earth map of the same site. Clear signatures of river, roads, urban and forested areas are observed.

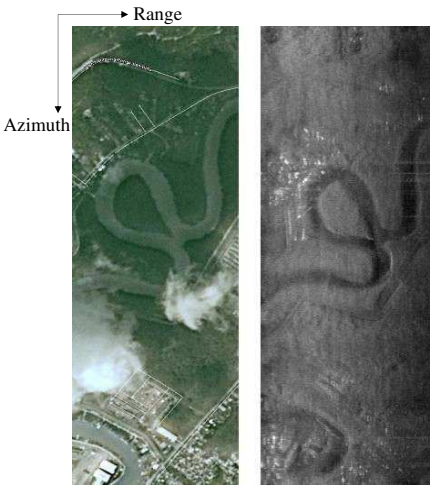

Figure 20. (a) Google earth map. (b) SAR image-1 at Mersing site.

Figure 21. (a) Google earth map. (b) SAR image-2 at Mersing site.

5. CONCLUSIONS

A miniature SAR system operated on a small UAV platform has been successfully designed and developed. Various design parameters have been carefully studied and determined in the system level design. Implementation of SAR system with especial attention to the dimension and size of the sensor chassis and antenna due to constrains of the UAV in particularly the limitation in weight and volume. A series of filed measurement and flight test has been conducted to verify the performance of the UAVSAR sensor. This new system will serve as a test-bed for demonstrating SAR technology and acquiring data for environmental monitoring in Malaysia.

ACKNOWLEDGMENT

This project is funded by Agency of Remote Sensing Malaysia under Ministry of Science, Technology and Innovation, Malaysia.

REFERENCES

1. Skolnik, M. I., *Radar Handbook*, McGraw-Hill, New York, 1970.
2. Curlander, J. C. and R. N. McDonough, *Synthetic Aperture Radar: System and Signal Processing*, A Wiley Interscience Publication, 1991.
3. Wiley, C. A., "Synthetic aperture radar — A paradigm for technology evolution," *IEEE Trans. on Aerospace and Electronic Systems*, Vol. 21, 440–443, 1985.
4. Ausherman, D. A., A. Kozma, J. L. Walkeretal, H. M. Jones, and E. C. Poggio, "Developments in radar imaging," *IEEE Trans. on Aerospace and Electronic Systems*, Vol. 20, No. 4, 363–440, 1984.
5. Ulaby, F. T., R. K. Moore, and A. K. Fung, *Microwave Remote Sensing-active and Passive*, Vol. 2, Addison Wesley, 1981.
6. Drinkwater, M. K., R. Kwok, and E. Rignot, "Synthetic aperture radar polarimetry of sea ice," *Proceeding of the 1990 International Geoscience and Remmote Sensing Symposium*, Vol. 2, 1525–1528, 1990.
7. Lynne, G. L. and G. R. Taylor, "Geological assessment of SIR-B imagery of the amadeus basin," *IEEE Trans. on Geosc. and Remote Sensing*, Vol. 24, No. 4, 575–581, 1986.
8. Hovland, H. A., J. A. Johannessen, and G. Digranes, "Slick detection in SAR images," *Proceeding of the 1994 International Geoscience and Remmote Sensing Symposium*, 2038–2040, 1994.
9. Walker, B., G. Sander, M. Thompson, B. Burns, R. Fellerhoff, and D. Dubbert, "A high-resolution, four-band SAR testbed with real-time image formation," *Proceeding of the 1986 International Geoscience and Remmote Sensing Symposium*, 1881–1885, 1996.
10. Storvold, R., E. Malnes, Y. Larsen, K. A. Høgda, S. E. Hamran, K. Müller, and K. A. Langley, "SAR remote sensing of snow parameters in Norwegian areas — Current status and future perspective," *Journal of Electromagnetic Waves and Applications*, Vol. 20, No. 13, 1751–1759, 2006.
11. Kong, J. A., S. H. Yueh, H. H. Lim, R. T. Shin, and J. J. van Zyl, "Classification of earth terrain using polarimetric synthetic aperture radar images," *Progress In Electromagnetics Research*, Vol. 3, 327–370, 1990.
12. Taylor, J. W. R., *Jane's Pocket Book of Remotely Piloted Vehicles*, Collier Books, New York, 1977.
13. Yong, J. M., *Secrets of Military Unmanned Aerial Vehicle*, Defense University Publisher, China, 2004.

14. Wall, R., *Trial Run: Sigint Version, Not Maritime Patrol, Attracts Initial German Interest in Global Hawk*, 42–43, McGraw-Hill, USA, 2003.
15. Zaugg, E. C., D. L. Hudson, and D. G. Long, "The BYU SAR: A small, student-built SAR for UAV operation," *The 2006 International Geoscience and Remote Sensing Symposium*, 411–414, 2006.
16. Hensley, S., K. Wheeler, G. Sadowy, et al., "Status of a UAVSAR designed for repeat pass interferometry for deformation measurements," *IEEE MTT-S International Microwave Symposium Digest*, 1453–1456, 2005.
17. Wheeler, K., S. Hensley, Y. Lou, T. Miller, and J. Hoffman, "An L band SAR for repeat pass deformation measurements on a UAV platform," *Proceedings of the IEEE Radar Conference*, 317–322, 2004.
18. Rosen, P. A., S. Hensley, K. Wheeler, G. Sadowy, T. Miller, S. Shaffer, R. Muellerschoen, C. Jones, H. Zebker, and S. Madsen, "UAVSAR: A new NASA airborne SAR system for science and technology research," *IEEE Conference on Radar*, 22–29, 2006.
19. Rosen, P. A., S. Hensley, K. Wheeler, G. Sadowy, T. Miller, S. Shaffer, R. Muellerschoen, C. Jones, and S. Madsen, and H. Zebker, "UAVSAR: Airborne SAR system for research," *IEEE A&E Systems Magazine*, 21–28, 2007.
20. Weib, M. and J. H. G. Ender, "A 3D imaging radar for small unmanned airplanes — ARTINO," *Radar Conference*, 209–212, 2005.
21. Weiss, M., O. Peters, and J. Ender, "A three dimensional SAR system on an UAV," *IEEE International Geoscience and Remote Sensing Symposium*, 5315–5318, 2007.
22. Wells, L., K. Sorensen, A. Doerry, and B. Remund, "Developments in SAR and IFSAR systems and technologies at sandia national laboratories," *IEEE Aerospace Conference Proceedings*, Vol. 2, 1085–1095, 2005.
23. Tsunoda, S. I., F. Pace, J. Stence, M. Woodring, W. H. Hensley, A. W. Doerry, and B. C. Walker, "Lynx: A high-resolution synthetic aperture radar," *IEEE Aerospace Conference Proceedings*, Vol. 5, 51–58, 2000.
24. Saldana, R. R. and F. P. Martinez, "Design of a millimetre synthetic aperture radar (SAR) onboard UAV's," *IEEE International Conference on Electronics, Circuits and Systems*, 1–5, 2007.
25. Peihong, R., "High-resolution 8 mm radar imaging technique,"

International Conference on Radar, 1–3, 2006.

26. Wissan, Y. V., I. Firmansyah, P. Rizki Akbar, J. T. Sri Sumantyo, and H. Kuze, "Development of circularly polarized array antenna for synthetic aperture radar sensor installed on UAV," *Progress In Electromagnetics Research C*, Vol. 19, 119–133, 2011.
27. Chan, Y. K., M. K. Azlindawaty, V. Gobi, B. K. Chung, and H. T. Chuah, "The design and development of airborne synthetic aperture radar," *IEEE International Geoscience and Remote Sensing Symposium*, Vol. 2, 518–520, Jul. 2000.
28. Koo, V. C., Y. K. Chan, V. Gobi, T. S. Lim, B.-K. Chung, and H.-T. Chuah, "The MASAR project: Design and development," *Progress In Electromagnetics Research*, Vol. 50, 279–298, 2005.
29. Chan, Y. K., B.-K. Chung, and H.-T. Chuah, "Transmitter and receiver design of an experimental airborne synthetic aperture radar sensor," *Progress In Electromagnetics Research*, Vol. 49, 203–218, 2004.
30. Gobi, V., B. K. Chung, and H. T. Chuah, "Design of a microstrip patch antenna for airborne SAR applications," *Journal of Electromagnetic Waves and Applications*, Vol. 19, No. 12, 1687–1701, 2005.
31. Chua, M. Y. and V. C. Koo, "FPGA-based chirp generator for high resolution UAV SAR," *Progress In Electromagnetics Research*, Vol. 99, 71–88, 2009.
32. International Telecommunication Union's (ITU) World Radiocommunication Conference 1997 (WRC-97).
33. Ulaby, F. T. and M. C. Dobson, *Handbook of Radar Scattering Statistics for Terrain*, Artech House, Norwood, 1989.
34. Cumming, I. G. and F. H. Wong, *Digital Processing of Synthetic Aperture Radar Data*, Artech House, Norwood, 2005.